Journal Name

RSCPublishing

ARTICLE

Luminescent Eu^{3+} doped $NaLa(WO_4)(MoO_4)$ and Ba_2CaMoO_6 prepared by the modified Pechini method

Cite this: DOI: 10.1039/xoxxooooox

Received ooth January 2012,
Accepted ooth January 2012

DOI: 10.1039/xoxxooooox

www.rsc.org/

M. Sletnes,[a] S. L. Skjærvø[a], M. Lindgren[b], T. Grande[a] and M-A. Einarsrud[a]

Modified Pechini synthesis routes were developed for synthesis of the novel red phosphor materials $NaLa(WO_4)(MoO_4):Eu^{3+}$ and $Ba_2CaMoO_6:Eu^{3+}$. Phase pure $NaLa(WO_4)(MoO_4):Eu^{3+}$ was obtained at calcination temperature ≥ 600 °C using malic acid or tartaric acid as complexing agents. Phase pure $Ba_2CaMoO_6:Eu^{3+}$ was attained using EDTA and citric acid, at calcination temperature ≥ 800 °C. Choice of complexing agents were discussed on the basis of precursor solubility, metal complex stability constants and conformations of the complexes. The powder properties were characterised using X-ray diffraction, thermal analysis and electron microscopy. Photoluminescence emission intensity was studied as a function of the complexing agents used and calcination temperature of the powders. Maximum emission intensity for $NaLa(WO_4)(MoO_4):Eu^{3+}$ was obtained at a calcination temperature of 600 °C.

Introduction

Development of new or improved synthesis routes to functional materials is important for the progress of sustainable energy technology. Wet chemical synthesis methods offer excellent control of important material properties, such as stoichiometry, homogeneity and crystal structure, as well as particle size and morphology, and are applicable to a wide range of materials. Here, a modified Pechini method is used to prepare phosphorescent oxides for application in white light emitting diodes (WLEDs).

WLEDs are very energy efficient compared to other white light sources, but "cold" light and poor colour rendering properties limit their attractiveness for general illumination. This can be improved by using a near ultraviolet (NUV) LED in combination with red, green and blue phosphors. Efficient green and blue phosphors already exist. However, the technology is limited by the lack of a stable and efficient red phosphor. A much researched group of novel red phosphor materials are the Eu^{3+} doped oxides of Mo and W, including compounds such as $Ca(W,Mo)O_4:Eu^{3+},Li^+$,[1, 2] $M^+M^{3+}(WO_4)_{2-x}(MoO_4)_x:Eu^{3+}$ (M^+ = Li, Na, K; M^{3+} = La, Gd, Y, Lu, Bi),[3-5] $M_6(W,Mo)O_{12}:Eu^{3+}$ (M = Y, Gd, Lu)[6-9] and $AB(W,Mo)O_6:Eu^{3+}$ (A = Ca, Sr, Ba; B = Mg, Ca).[10-18] The first two compounds crystallize in the scheelite structure, where there is enhancement of NUV excitation due to non-centrosymmetric lattice sites. $M_6(W,Mo)O_{12}:Eu^{3+}$ (M = Y, Gd, Lu) and $AB(W,Mo)O_6:Eu^{3+}$ (A = Ca, Sr, Ba; B = Mg, Ca) crystallize in structures with MoO_6 groups, where the NUV excitation is enhanced via energy transfer from the host material. The most common synthesis route for these materials is solid state reaction,[3, 10-13, 17, 19] mainly because of the simplicity of the method, such as no need for soluble precursors or advanced equipment. However, several grindings and re-firings are often necessary to achieve phase purity, and the process readily introduces impurities and defects which would reduce luminous efficacy.[20]

Pechini-type sol-gel synthesis is highly suitable for fabrication of phosphor materials due to its versatility and ability to produce powders of high homogeneity and purity at relatively low temperatures. Thus, there are several reports of modified Pechini synthesis of scheelite structured molybdate/tungstate phosphor materials.[21-25] Zhang et al. synthesised 6-coordinated $(Sr_{0.98-x}Ba_xEu_{0.02})_2Ca(Mo_{1-y}W_y)O_6$ by a modified Pechini route, however, the Raman spectroscopy data strongly suggests that there were secondary phases present in the material.[16] Very recently, Li and Liu also reported synthesis of $Ba_2CaMoO_6:Eu^{3+}$ by a Pechini route using citric acid as a complexing agent and a calcination temperature of 1100 °C.[26] The paper focused more on optical properties than the actual synthesis. Thus optimisation of synthesis parameters were not discussed, and it is difficult to determine from the published data whether complete phase purity was obtained. Here we report the synthesis of phase pure $NaLa(WO_4)(MoO_4):Eu^{3+}$ and $Ba_2CaMoO_6:Eu^{3+}$ by the modified Pechini method, with optimisation of important synthesis parameters such as

complexing agents, pH and calcination temperatures. The relationship between phase purity and complexing agents are discussed with a basis in metal complex stability constants and conformations of the complexes.

Experimental

All the precursors were bought from Sigma Aldrich. $La(NO_3)_3 \cdot 6\ H_2O$ (99.9 %), $Eu(NO_3)_3 \cdot 6H_2O$ (99.9 %), KNO_3 (≥ 99.0 %), H_2WO_4 (99.0 %), $(NH_4)_6Mo_7O_{24} \cdot 4H_2O$ (99.98 %), $Ca(NO_3)_2 \cdot 4H_2O$ (≥ 99.0 %), malic acid (MA, 99.0 %), DL-tartaric acid (TA, 99%), citric acid (CA, 99 %), ethylenediaminetetraacetic acid (EDTA, ≥ 99 %), diethylenetriaminepentaacetic acid (DTPA, ≥ 99.0 %) and ethylene glycol (EG, ≥ 99.5 %) were used without further purification. $NaNO_3$ (99.0 %) and $Ba(NO_3)_2$ (≥ 99 %) were dried at 200 °C for at least 12 h prior to use. The concentrations of cation precursor solutions were determined using thermogravimetric standardisation. A flow chart of the synthesis route to $NaLa(WO_4)(MoO_4):Eu^{3+}$ is presented in Figure 1. Precursor solutions of $La(NO_3)_3 \cdot 6H_2O$ (~ 0.3 mol La per g solution), H_2WO_4 (~ 0.2 mol W per g solution) and $(NH_4)_6Mo_7O_{24} \cdot 4H_2O$ (~ 0.6 mol Mo per g solution) complexed with MA or TA in a 1:1 ratio with the cations were prepared and standardised. The tungstate solution was made with a basis in the route developed by Gil et al.[27] The precursor solutions were mixed in the order W (0.01 mol), Mo (0.01 mol) and then La (0.0096 mol). $NaNO_3$ (0.0096 mol) and $Eu(NO_3)_3 \cdot 6H_2O$ (0.0008 mol) were added along with an additional amount of complexing agent to give a cation to complexing agent ratio of 1:1. EG (0.04 mol) was added to some of the syntheses, as shown in Table 1. The solutions were heated to 100 °C on a hot-plate and as the water content became critically low, the gels self-ignited initiating smoldering reactions.

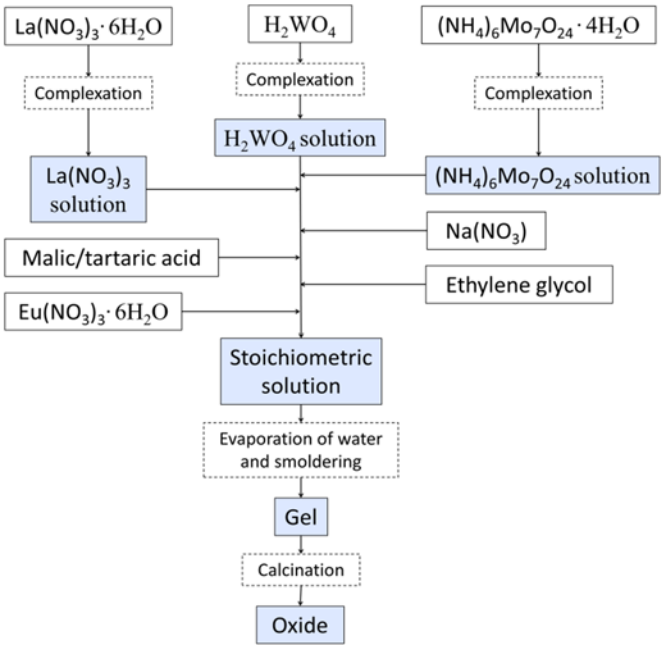

Figure 1 A flow chart of the synthesis route to $NaLa(WO_4)(MoO_4):Eu^{3+}$.

Table 1 Combinations of complexing and polymerisation agents investigated in the synthesis of $NaLa(WO_4)(MoO_4):Eu^{3+}$.

Complexing agent(s)	Ethylene glycol
Malic acid	No
Malic acid	Yes
Tartaric acid	No
Tartaric acid	Yes

The cool and dry gels were crushed into homogeneous powders in an agate mortar before they were calcined in air at 300, 400, 500, 600, 700 and 1000 °C.

A flow chart showing the synthesis of $Ba_2CaMoO_6:Eu^{3+}$ is given in Figure 2. Preliminary experiments[28] were carried out without addition of the Eu^{3+} dopant in order to find suitable complexing agents, molar ratios of complexing agents to cations, pH values and calcination temperatures. The investigated complexing agents were MA, TA, CA, EDTA and DTPA. EG was used as a polymerization agent in some of the syntheses. The complexing agents were dissolved in water and the pH was adjusted with NH_3 solution (25 %). Stoichiometric amounts of $Ca(NO_3)_2 \cdot 4H_2O$ and $(NH_4)_6Mo_7O_{24} \cdot 4H_2O$ were added in the form of precursor solutions of approximately $5 \cdot 10^{-4}$ mol cations/g. $Ba(NO_3)_2$ was dissolved in the solution, EG was added, and the water was slowly evaporated at 120 °C on a hotplate until a viscous/sticky gel was obtained. The gel was partly decomposed at 200 °C for 12 h. The resulting materials were calcined in air at 550, 600, 700 or 1100 °C for 6 h. Based on the preliminary experiments, DTPA, CA, and CA in combination with either EDTA or DTPA were chosen for the synthesis of Eu^{3+} doped Ba_2CaMoO_6. An overview of the syntheses with pH values and complexing agent to cation ratio is shown in Table 2. EG was not used in any of the syntheses of Eu^{3+} doped samples.

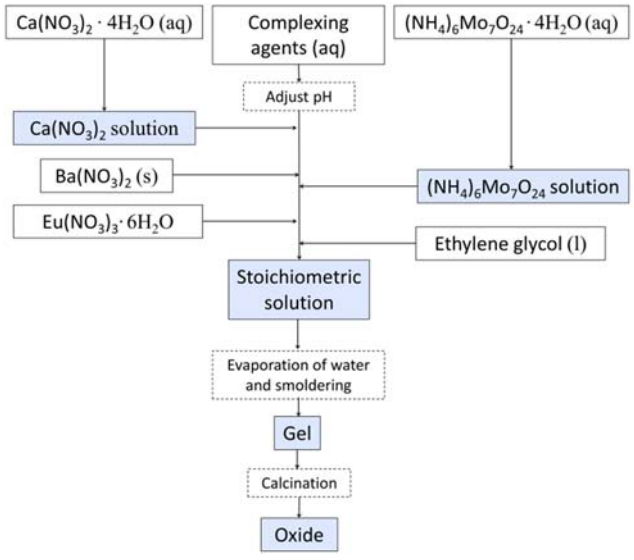

Figure 2 A flow chart of the synthesis route to Ba_2CaMoO_6.

Table 2 Combinations of complexing agents and pH values investigated in the synthesis of $Ba_2CaMoO_6:Eu^{3+}$.

Complexing agent(s)	Ratio to cations	pH
CA, EDTA	2, 1	8.0
CA, DTPA	2, 1	8.0
DTPA	1	7.0

Thermogravimetric analysis (TGA) and differential scanning calorimetry (DSC) were performed on the ground gels (after smoldering) using a Netzsch STA 449C Jupiter in synthetic air. The $NaLa(WO_4)(MoO_4)$ gels were analysed up to 1000 °C with a heating rate of 10 °C/min. The Ba_2CaMoO_6 gels were analysed up to 1100 °C with a heating rate of 5 °C/min. The crystal structure and phase composition of the phosphors were studied by X-ray powder diffraction (XRD) using a Bruker AXS D8 Focus equipped with a LynxEye™ detector and a Cu-radiation source ($CuK\alpha_{1,2}$) with Bragg Brentano geometry. Crystallite sizes were estimated from the XRD data using the Scherrer equation.[29] Scanning electron microscopy (SEM) was performed in a Hitachi S-5500 S (in-lens) ultra-high resolution S(T)EM. BET surface area was calculated from nitrogen gas adsorption (Micromeritics Tristar 3000) on powder samples. The average particle sizes of the powders were estimated from the BET surface areas by assuming spherical particles. The photoluminescence (PL) excitation spectra were measured using a Horiba Jobin-Yvon Fluorolog-3 spectrofluorimeter with a Xenon lamp as an excitation source and a model R928P (photomultiplier tube) Hamamatsu detector. The powders were pressed into discs with a diameter of 13 mm, and mounted on a custom made sample holder. Emission spectra were measured using a Leica DM5500 B fluorescence microscope, and integrated emission intensities were numerically calculated using the trapz function in Matlab.

Results

Single-phase Eu-doped $NaLa(WO_4)(MoO_4)$ powders were obtained for all the synthesis routes with calcination temperatures ≥ 600 ºC, as evidenced by XRD. The crystal structure was Scheelite ($I4_1/a$) with lattice parameters a = 5.341 and c = 11.695 Å, which is in good agreement with the literature on $NaLa(WO_4)_2$ (a = 5.349, b = 11.628 Å)[30] and $NaLa(MoO_4)_2$ (a = 5.342, b = 11.738)[31]. Evolution of the X-ray diffractograms with calcination temperature is shown in Figure 3 for the synthesis with TA as a complexing agent. The same trend was found for all the other combinations of complexing agents, except using MA without EG, where precipitation of one or more crystalline phases occurred in the gel. The appearance of the crystalline compound(s) diminished significantly upon calcination at 300 °C. The crystalline phase(s) could not be identified, but the low decomposition temperature indicates that it was an organic salt. The diffractograms after calcination at 400 and 500 °C demonstrated formation of phase pure $NaLa(WO_4)(MoO_4)$. However, the grey colour of the powders as well as TGA indicated that the organic materials in the gel were not completely decomposed at these calcination temperatures. No substantial mass loss was observed by TGA after 600 °C for any of the gels. The crystallite sizes determined by the Scherrer equation were about 20, 30 and 45 nm after calcination at 600, 700 and 1000 °C, respectively.

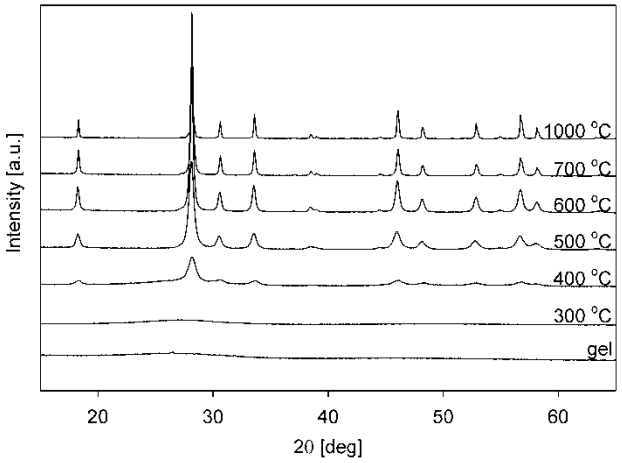

Figure 3 XRD patterns of $NaLa(WO_4)(MoO_4):Eu^{3+}$ synthesised using tartaric acid as a complexing agent. Calcination temperatures are included in the figure.

Phase pure Ba_2CaMoO_6 was achieved with DTPA and with CA in combination with EDTA at a calcination temperature of 1100 °C, and thus these complexing agents were chosen for further development of the synthesis route. TGA and DSC of gels made with DTPA (1:1 ratio with cations), CA (3:1), and CA in combination with EDTA (2:1:1) are shown in Figure 4. The main weight loss occurred below 550 °C, and was due to evaporation of absorbed water, and decomposition of the nitrates and organic gel network. The largest weight loss was accompanied by a sharp exothermic peak in the DSC curve, centred at 480 °C for CA, 510 °C for CA-EDTA, and 540 °C for DTPA, indicating the main combustion of the chelate complexes along with the formation of metal oxides. The final weight loss occurred between 710 and 770 °C, and was presumably related to decomposition of carbonate intermediates. The final weight loss occurred at a lower temperature for the CA-EDTA combination than for the other complexing agents. Although the TGA curve did not show any weight loss after 800 °C, the DSC curve indicated that an exothermic process was active until 1050 °C. This may be due to final ordering and crystallization of the perovskite material.

Figure 5a shows the XRD patterns of 2 mol% Eu^{3+} doped Ba_2CaMoO_6 synthesised using DTPA (1:1 ratio with cations), CA in combination with EDTA (2:1:1) and CA in combination with DTPA (2:1:1) as complexing agents, calcined at 700, 800 and 1100 °C. The crystal structure of the main phase was cubic perovskite (Fm-3m) with lattice parameter a = 8.379 Å, corresponding well with published crystallographic data for Ba_2CaMoO_6 (a = 8.355 Å)[32].

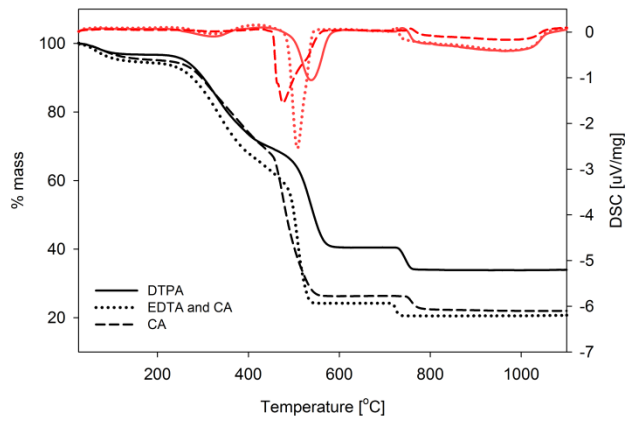

Figure 4 TGA and DSC curves of Ba_2CaMoO_6 precursor gels with three different complexing agents.

A small amount of $BaMoO_4$ secondary phase was observed, evidenced by the reflection at $2\theta \approx 27°$ for the samples calcined at 700 °C. However, all the syntheses except for the one with a combination of CA and DTPA yielded phase pure Ba_2CaMoO_6 after calcination at 800 and 1100 °C. Calcination of the precursor gels at 1100 °C resulted in higher phase purity than at 700 °C, but also significant grain growth and coarsening, as seen in the SEM images of Eu^{3+} doped Ba_2CaMoO_6 in Figure 5 b and c. Estimated average particle size from BET surface area increased from 280 nm when the calcination temperature was 700 °C to 2.4 µm at 1100 °C.

The exciation and emission spectra of $NaLa(WO_4)(MoO_4):Eu^{3+}$ are shown in Figure 6**.** The red area marks the wavelength range for NUV LED emission, and thus the range where the phosphor should easily be excited. The broad excitation band centred at ~260 nm is due to the O-W/Mo charge transfer. The other excitation peaks originate from the intra-configurational 4f–4f transitions of Eu^{3+} from the ground state $^7F_0$ to the excited state $^5L_6$, $^5D_2$ and $^5D_1$. The main emission line originates from the forced electric dipole transition, $^5D_0$ -$^7F_2$. Both the high relative intensity of the intra-configurational transitions of Eu^{3+} compared to the charge transfer (CT) band, and the domination of $^5D_0$-$^7F_2$ in the emission spectrum are clear evidence of Eu^{3+} in non-centrosymmetric lattice sites.[33] The integrated PL emission intensities of the 8 mol% Eu^{3+} doped $NaLa(WO_4)(MoO_4)$ is plotted as a function of calcination temperature in Figure 7. The highest PL intensity was achieved for the powders calcined at 600 °C for both complexing agents, and the maximum intensity was slightly higher for tartaric acid than malic acid.

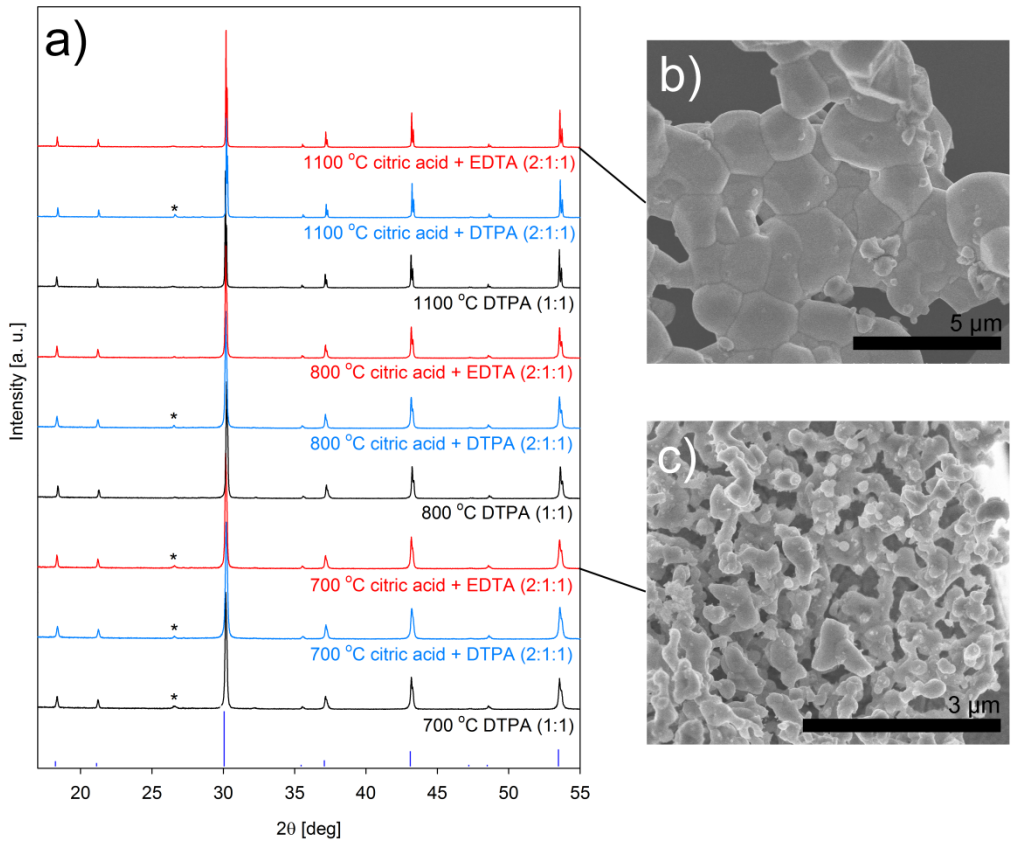

Figure 5 XRD patterns of Ba_2CaMoO_6 synthesised by the modified Pechini method. Calcination temperatures and complexing agents are included in the figure, with the ratio of complexing agents to cations in parentheses. An asterisk indicates peaks originating from a $BaMoO_4$ secondary phase, and a reference pattern for Ba_2CaMoO_6 [32] is included. b) SEM images of $Ba_2CaMoO_6:Eu^{3+}$ powder produced by modified Pechini synthesis with CA and EDTA as complexing agents calcined at 700 and c) 1100 °C.

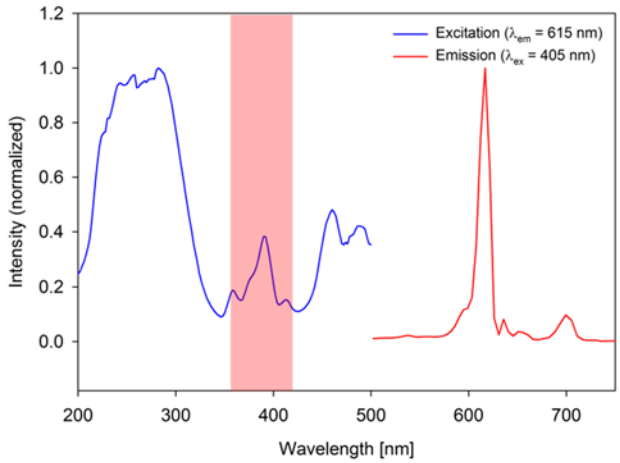

Figure 6 Excitation and emission spectrum of $NaLa(WO_4)(MoO_4):Eu^{3+}$. The red area marks the range for NUV LED emission.

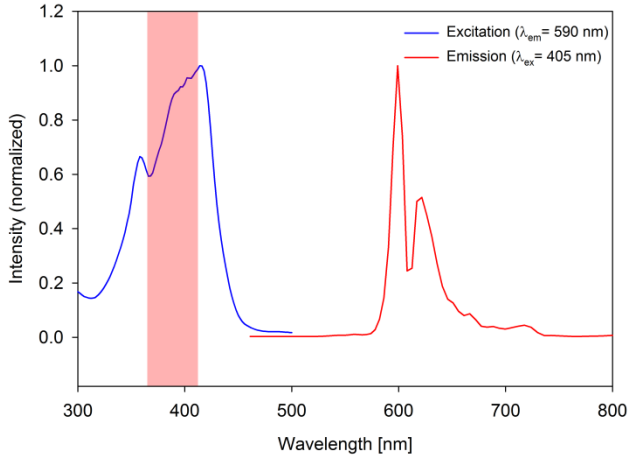

Figure 8 Excitation and emission spectrum of Ba2CaMoO6:Eu3+. The red area marks the range for NUV LED emission.

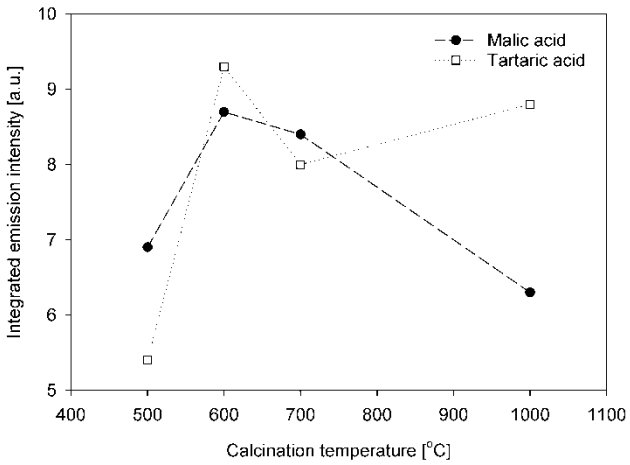

Figure 7 Integrated PL emission intensities of the 8 mol% Eu^{3+} doped $NaLa(WO_4)(MoO_4)$ synthesized with different complexing agents as a function of calcination temperature. The excitation wavelength was 405 nm.

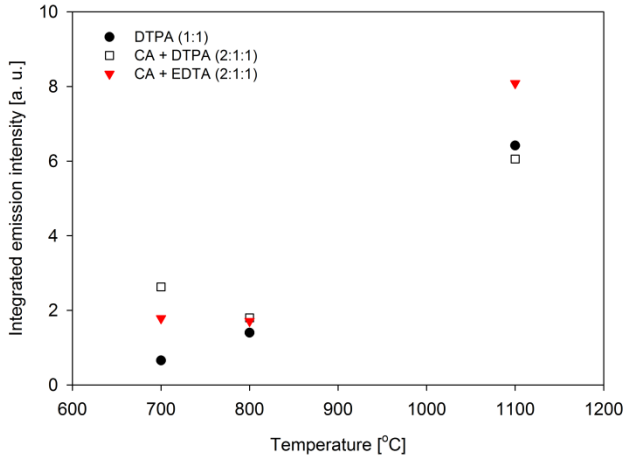

Figure 9 Integrated PL emission intensities of the 2 mol% Eu^{3+} doped Ba_2CaMoO_6 synthesized with different complexing agents as a function of calcination temperature. The excitation wavelength was 405 nm.

Figure 8 displays the excitation and emission spectra of $Ba_2CaMoO_6:Eu^{3+}$. The broad MoO_6 charge transfer band in the ultraviolet allows efficient NUV excitation. Two main peaks were observed in the emission spectra, centred at 595 nm ($^5D_0$ - $^7F_1$) and 615 nm ($^5D_0$ -$^7F_2$). Transitions from $^5D_0$ to $^7F_3$ and $^7F_4$ were also noticeable as weak emission peaks on the low energy side of the spectra. The dominating emission line originates from the magnetic dipole transition, $^5D_0$ -$^7F_1$, indicating Eu^{3+} in centrosymmetric lattice sites. The integrated photoluminescence (PL) emission intensities of the 2 mol% Eu^{3+} doped Ba_2CaMoO_6 synthesized with different complexing agents is plotted as a function of calcination temperature in Figure 9. No significant difference in emission intensity of the samples calcined at 700 and 800 °C was observed. However, calcination at 1100 °C led to a fourfold increase in emission intensity. The highest emission intensity was observed for the synthesis with a combination of CA and EDTA.

Discussion

Single-phase Eu-doped $NaLa(WO_4)(MoO_4)$ was produced with calcination temperatures as low as 600 °C, establishing the ease of making high quality powders with the modified Pechini method. All the complexing agents gave single phase materials at these temperatures. However, observation of crystalline phase(s) in the gels made with malic acid as the only complexing agent, suggests that tartaric acid or malic acid in combination with ethylene glycol are better choices for the synthesis of Eu-doped $NaLa(WO_4)(MoO_4)$.

The synthesis of Ba_2CaMoO_6 proved to be more challenging. Precipitation of $Ba(NO_3)_2$ was observed upon evaporation of water before gelation when MA or TA were used as complexing agents. Increasing the molar ratio of complexing agent to cations to 3:1 reduced the amount of precipitation, but did not completely eliminate it. When EDTA was used as the

only complexing agent, XRD analysis of the gels also showed that precipitation had occurred. In this case, the precipitate was not readily identified, and was assumed to be an organic salt based on EDTA or its decomposition products. Adjusting the pH and EDTA to cation ratio did not eliminate the precipitation. CA (3:1 ratio with cations), DTPA (1:1) and CA and EDTA in combination (2:1:1) resulted in amorphous gels. None of the preliminary experiments yielded phase pure Ba_2CaMoO_6 after calcination at 550, 600 or 700 °C. Commonly observed secondary phases were $Ba_{1-x}Ca_xCO_3$ and $BaMoO_4$. Phase pure material was obtained by using either DTPA or EDTA in combination with CA and calcination temperatures ≥ 800 °C.

The difference in the required complexing agents for the synthesis of the two materials can be explained partly by the solubility of the precursors and stability of the cation complexes. The stability constants for complexes with Na^+, La^{3+}, Ca^2 and Ba^{2+} are plotted in Figure 10. The stability constants are significantly higher for EDTA and DTPA than for MA, TA and CA, and the stability increases in the order $Na^+<Ba^{2+}<Ca^{2+}<La^{3+}$. Furthermore, the solubility of $NaNO_3$ is about 10 times higher than $Ba(NO_3)_2$, and hence strong complexation may not be necessary to avoid precipitation of $NaNO_3$. Thus it was possible to synthesise $NaLa(WO_4)(MoO_4)$ using weaker complexing agents than Ba_2CaMoO_6.

Phase pure Ba_2CaMoO_6 was only obtained with EDTA when in combination with CA, whereas DTPA resulted in phase pure material without addition of CA. Since EDTA is a hexadendate ligand, it can form up to 6 bonds with a metal cation. DTPA is potentially an octadentate ligand, but typically forms less than 8 bonds with most metal cations, leaving one or two sites available for bonding with other reagents.[34, 35] Hence this can explain why DTPA proved to be a better complexing agent than EDTA when not combined with CA.

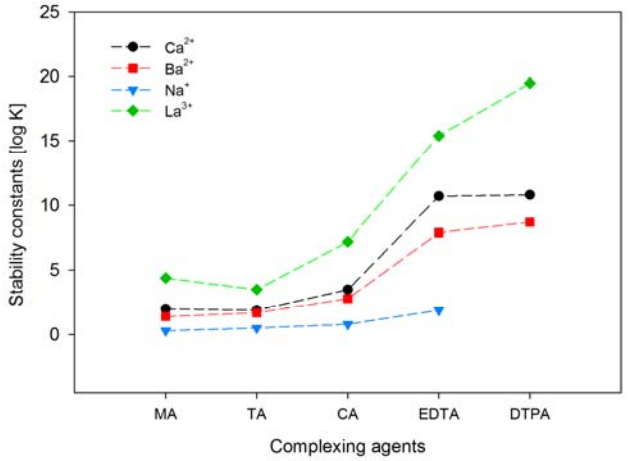

Figure 10 Stability constants (log K) of complexes of Ca^{2+}, Ba^{2+}, Na^+ and La^{3+} with malic acid, tartaric acid, citric acid, EDTA and DTPA. Based on data from reference [36]. The dotted lines are a guide to the eye.

There are several sol-gel syntheses of perovskites reported in the literature in which EDTA and CA are used in combination, and many of them involve basic cations, such as Sr, Ba and La [37-42]. The interaction of EDTA and CA is clearly favourable for the formation of metal-organic precursor gels for these perovskite materials, although the mechanism is not completely understood. It is interesting to note that the TGA of the Ba_2CaMoO_6 gels (Figure 4) showed that the final weight loss occurred at a lower temperature for the EDTA-CA combination than for CA alone. It has previously been shown by Abdullah et al. that in the sol-gel synthesis of $BaCe_{0.54}Zr_{0.36}Y_{0.1}O_{2.95}$, gels prepared with an EDTA-CA combination exhibited lower thermal decomposition temperatures than gels prepared with EDTA or CA alone.[37] It was argued that the combination acted as a better combustion reagent to increase the reaction rate. As in our synthesis, Abdullah et al. did not observe any weight loss by TGA after 750 °C, but 1100 °C was necessary to obtain phase purity. Feldhoff et al. have shown that the synthesis of $(Ba_{0.5}Sr_{0.5})(Fe_{0.8}Zn_{0.2})O_{3-\delta}$ perovskites by the EDTA-CA sol-gel route involves nanoscale solid state reactions between carbonate and oxide intermediate phases.[39] This is in agreement with our observations of $BaCO_3$ and tetragonal molybdates for calcination temperatures ≤ 700 °C. The details of the reaction phases and mechanisms of such systems are highly complex, and the mixture of complexing agents could possibly be determining for the compositions of any nanoscale intermediate phases.

Based on the XRD and PL results, the synthesis route using a combination of EDTA and CA, and a calcination temperature of 1100 °C was the best choice for the synthesis of $Ba_2CaMoO_6:Eu^{3+}$. The fact that DTPA is a suspected human reproductive toxicant was also in favour of choosing the EDTA-CA route. Once the optimized synthesis parameters had been obtained for the synthesis of $Ba_2CaMoO_6:Eu^{3+}$, the synthesis route could easily be adapted to synthesise compounds in the Eu^{3+}-doped $(Sr,Ba)_2Ca(W,Mo)O_6$ series.

The emission of $NaLa(WO_4)(MoO_4):Eu^{3+}$, which was mainly concentrated at 615 nm, is perfect for phosphor converted WLEDs with high luminous efficiency.[43] However, the relatively narrow lines in the NUV part of the excitation spectrum are not ideal for WLED application. The emission spectrum of the pumping LED changes slightly due to variations in the driving current and/or the junction temperature. To keep the emission colour of the WLED stable, it is important that the excitation spectrum of the phosphors are broad and flat enough to compensate for the variation in pumping wavelengths. It is very interesting to note that the highest PL emission intensity for $NaLa(WO_4)(MoO_4):Eu^{3+}$ was achieved at a calcination temperature of only 600 °C. This corresponds to the lowest calcination temperature which resulted in phase pure material, since the organic components of the gel were not completely decomposed at 500 °C. Usually one would expect the PL intensity to increase with increasing calcination temperature due to higher crystallinity and

decreased surface area. The crystallite size after calcination at 600 °C was only about 20 nm, and the optical properties may be influenced by final size effects which are yet to be understood. Increased PL emission intensity in combination with smaller particle size is very interesting for WLED phosphors since using nanosized particles will eliminate efficiency loss due to scattering.[20]

The excitation spectrum of $Ba_2CaMoO_6:Eu^{3+}$displayed a broad CT band in the NUV, and should thus provide the required emission stability under varying conditions. However, the main emission was concentrated at 595 nm, which does not give the optimal red colour purity for phosphor converted WLEDs. Substituting Sr for Ba results in lowering of the perovskite lattice symmetry, while substituting W for Mo broadens and shifts the CT band.[17] Thus playing with the composition could allow for optimisation of the optical properties. The modified Pechini synthesis route developed in this work would be ideal for such a task since it allows strict control of the stoichiometry, homogeneity and phase purity.

Conclusions

Phase pure $NaLa(WO_4)(MoO_4):Eu^{3+}$ and $Ba_2CaMoO_6:Eu^{3+}$ were synthesised by newly developed modified Pechini routes. Both materials displayed desirable optical properties for use as phosphors in WLEDS, and low calcination temperatures resulted in increased emission intensity for $NaLa(WO_4)(MoO_4):Eu^{3+}$. The different complexing agents chosen for the synthesis of the two materials was explained and discussed with respect to the solubility of the precursors and stability of the cation complexes. This insight enables to simplify the design of modified Pechini routes to related oxide materials.

Acknowledgements

The work was funded by The Norwegian University of Science and Technology within the strategic research area MATERIALS.

Notes and references

[a] Department of Materials Science and Engineering, Norwegian University of Science and Technology, NO-7491 Trondheim, Norway.

[b] Department of Physics, Norwegian University of Science and Technology, NO-7491 Trondheim, Norway.

1. A. Xie, X. M. Yuan, S. J. Hai, J. J. Wang, F. X. Wang and L. Li, *J. Phys. D: Appl. Phys.*, 2009, **42**, 105107.
2. C. Q. Zhu, S. G. Xiao, B. W. Ding, X. L. Yang and R. F. Qiang, *Mater. Sci. Eng., B*, 2008, **150**, 95-98.
3. S. Neeraj, N. Kijima and A. K. Cheetham, *Chem. Phys. Lett.*, 2004, **387**, 2-6.
4. L. Li, J. Zhang, W. Zi, S. Gan, G. Ji, H. Zou and X. Xu, *Solid State Sci.*, 2014, **29**, 58-65.
5. L. L. Li, L. Liu, W. W. Zi, H. Yu, S. C. Gan, G. J. Ji, H. F. Zou and X. C. Xu, *J. Lumin.*, 2013, **143**, 14-20.
6. H. Y. Li, H. M. Noh, B. K. Moon, B. C. Choi, J. H. Jeong, K. Jang, H. S. Lee and S. S. Yi, *Inorg. Chem.*, 2013, **52**, 11210-11217.
7. H. Li, H. K. Yang, B. K. Moon, B. C. Choi, J. H. Jeong, K. Jang, H. S. Lee and S. S. Yi, *Inorg. Chem.*, 2011, **50**, 12522-12530.
8. H. Li, H. K. Yang, B. K. Moon, B. C. Choi, J. H. Jeong, K. Jang, H. S. Lee and S. S. Yi, *J. Mater. Chem.*, 2011, **21**, 4531-4537.
9. Y. Tian, B. J. Chen, R. N. Hua, H. Y. Zhong, L. H. Cheng, J. S. Sun, W. L. Lu and J. Wan, *Physica B*, 2009, **404**, 3598-3601.
10. S. Ye, Y. J. Li, D. C. Yu, Z. M. Yang and Q. Y. Zhang, *J. Appl. Phys.*, 2011, **110**, 013517.
11. V. Sivakumar and U. V. Varadaraju, *Electrochem. Solid-State Lett.*, 2006, **9**, H35-H38.
12. V. Sivakumar and U. V. Varadaraju, *J. Electrochem. Soc.*, 2007, **154**, J28-J31.
13. V. Sivakumar and U. V. Varadaraju, *J. Solid State Chem.*, 2008, **181**, 3344-3351.
14. F. Lei and B. Yan, *J. Optoelectron. Adv. Mater.*, 2008, **10**, 158-163.
15. S. Li, X. T. Wei, K. M. Deng, X. N. Tian, Y. G. Qin, Y. H. Chen and M. Yin, *Curr. Appl. Phys.*, 2013, **13**, 1288-1291.
16. L. Zhang, P. Han, Y. Han, Z. Lu, H. Yang, L. Wang and Q. Zhang, *J. Alloys Compd.*, 2013, **558**, 229-235.
17. S. Ye, C. H. Wang, Z. S. Liu, J. Lu and X. P. Jing, *Appl. Phys. B*, 2008, **91**, 551-557.
18. S. Ye, C.-H. Wang and X.-P. Jing, *J. Electrochem. Soc.*, 2008, **155**, J148-J151.
19. Z. Wang, H. Liang, M. Gong and Q. Su, *J. Alloys Compd.*, 2007, **432**, 308-312.
20. S. Ye, F. Xiao, Y. X. Pan, Y. Y. Ma and Q. Y. Zhang, *Mater. Sci. Eng., R*, 2010, **71**, 1-34.
21. A. Zalga, Z. Moravec, J. Pinkas and A. Kareiva, *J. Therm. Anal. Calorim.*, 2011, **105**, 3-11.
22. F. B. Cao, L. S. Li, Y. W. Tian, Y. J. Chen and X. R. Wu, *Thin Solid Films*, 2011, **519**, 7971-7976.
23. J. L. Lei, Y. Yu, L. J. Li, S. B. Cheng, G. Y. Li and N. B. Li, *J. Rare Earths*, 2012, **30**, 330-334.
24. F.-B. Cao, L.-S. Li, Y.-W. Tian, Z.-F. Gao, Y.-J. Chen, L.-J. Xiao and X.-R. Wu, *Opt. Mater.*, 2011, **33**, 751-754.
25. H. Xie, F. Li, H. Xi, R. Tian and X. Wang, *J Mater Sci: Mater Electron*, 2015, **26**, 23-31.
26. Y. Li and X. Liu, *Opt. Mater.*, 2015, **42**, 303-308.
27. V. Gil, R. A. Strom, L. J. Groven and M. A. Einarsrud, *J. Am. Ceram. Soc.*, 2012, **95**, 3403-3407.
28. M. Sletnes, PhD Thesis, "Wet chemical synthesis of silicon nanoparticles and phosphorescent oxides for white light emitting diodes" Norwegian University of Science and Technology, 2014. ISSN: 1503-8181.
29. A. L. Patterson, *Phys. Rev.*, 1939, **56**, 978-982.
30. H. Li, G. Hong and S. Yue, *Zhongguo Xitu Xuebao (J. Chin. Rare Earth Soc.)*, 1990, **8**, 37-41.
31. R. Teller, *Acta Crystallogr. C*, 1992, **48**, 2101-2104.
32. E. G. Steward and H. P. Rooksby, *Acta Crystallogr.*, 1951, **4**, 503.
33. G. S. Ofelt, *J. Chem. Phys.*, 1962, **37**, 511-520.
34. C. Sadun, R. Bucci and A. L. Magri, *J. Am. Chem. Soc.*, 2002, **124**, 3036-3041.
35. V. L. Silva, R. Carvalho, M. P. Freitas, C. F. Tormena and W. C. Melo, *Spectrochim. Acta A*, 2007, **68**, 1197-1200.
36. A. E. Martell, R. J. Motekaitis and R. M. Smith, *Critically selected stability constants of metal complexes database: Version 8. (NIST Database 46)*, Available for download at http://www.nist.gov/srd/nist46.cfm (May 4th 2014).
37. N. A. Abdullah, S. Hasan and N. Osman, *J. Chem.*, 2013 Article ID 908340, 7.
38. X. F. Ding, Y. J. Liu, L. Gao and L. Guo, *J. Alloys Compd.*, 2008, **458**, 346-350.
39. A. Feldhoff, M. Arnold, J. Martynczuk, T. M. Gesing and H. Wang, *Solid State Sci.*, 2008, **10**, 689-701.
40. C. Jeong, J. Ryu, T. Noh, Y. N. Kim and H. Lee, *Adv. Appl. Ceram.*, 2013, **112**, 494-498.
41. H. Patra, S. K. Rout, S. K. Pratihar and S. Bhattacharya, *Powder Technol.*, 2011, **209**, 98-104.
42. D. H. Prasad, S. Y. Park, E. O. Oh, H. Ji, H. R. Kim, K. J. Yoon, J. W. Son and J. H. Lee, *Appl. Catal., A*, 2012, **447**, 100-106.
43. P. F. Smet, A. B. Parmentier and D. Poelman, *J. Electrochem. Soc.*, 2011, **158**, R37-R54.